Properties of Graphene and Boron Nitride

Coco Kern, Elsa Schönwiese, Jiaqi Zhou, Shayan Shaterpoori, Ronghao Yin

March 2024

Abstract

Since being discovered in 2004 [1], graphene has proven to have properties which exceed that of materials, which are thought to be very high in that category. It has extremely high electron mobility , thermal conductivity tensile strength. This makes graphene an excellent conductor of electricity and heat and also very strong. These properties arise from the simple layout of the graphene lattice in its honeycomb structure. We shall analytically show how the geometry of the lattice leads to some of these properties, specifically, the superconductivity. Boron nitride, made from two atoms, unlike graphene, will also be analysed and compared to graphene regarding the nearest neighbour Hamiltonian and the dispersion.

Contents

1 Introduction

Graphene is a single sheet, a plane layer of carbon atoms bounded together in a honeycomb lattice. Within systems composed solely of carbon atoms, graphene, a two-dimensional carbon allotrope, plays a pivotal role by serving as a foundational element for understanding electronic properties across various carbon allotropes [2].

The remarkable electronic characteristics of single and bi-layer graphene are particularly striking and unexpected, and this report will highlight some of them. Additionally, graphene exhibits notable properties in gas adsorption, magnetism, and electrochemistry, and its response to doping by electrons and holes is equally remarkable [3]. Graphene has been tested for a wide range of applications such as transparent conductive films, ultra-sensitive chemical sensors, thin-film transistors, quantum dot devices and anti-corrosion coverings [4].

Apart from all the possibilities graphene offers for technological applications, it offers much promise even in fundamental research. Firstly, the existence of 2D crystals has been questioned, as suggested by the Mermin-Wagner theorem, which claims that 2D crystals lose their long-range order, resulting in melting at small but non-zero temperatures due to thermal fluctuations. Nevertheless, Graphene is the first 2D crystal observed in nature. Additionally, the electron cloud, which bounds each carbon atom to its nearest neighbours with a distance of 0.142 nm, raised questions about graphene's quantum mechanical properties [4].

Furthermore, electrons in graphene exhibit relativistic behaviour, rendering the system an excellent candidate for testing quantum field theoretical models in high-energy physics. Electrons in graphene can be interpreted as massless charged fermions in two-dimensional space, a particle typically unobservable in our three-dimensional world, as all massless elementary particles, like photons and neutrinos, are electrically neutral. Graphene then serves as a link between condensed matter and high-energy physics [5]. Section 2.4 will directly link the Hamiltonian of graphene and a massless spin 1/2 particle.

Additionally, we conduct some research on the 2D hexagonal boron nitride since the affinity between graphene and hexagonal BN extends significantly as both share a similar hexagonal 'honeycomb' lattice structure. Due to its insulating characteristics, hexagonal BN is frequently regarded as the optimal base for graphene's conductivity[6]. In section 3, we compare hexagonal boron nitride with graphene to see their differences and similarities. Hence, this discussion of Graphene starts with a discussion of its elementary electronic properties.

2 Elementary Electronic Properties of Graphene

2.1 Graphene's Lattice Structure

As graphene's lattice structure is of a honeycomb form, we start our investigation by understanding how the honeycomb form comes to be. Because graphene is a single sheet of Carbon (C) atoms bounded together, the properties of the carbon atom determine this structure. The electronic structure of an isolated C atom is $(1s)^2(2s)^2(2p)^4$. The $1s$ remains immobile in a solid-state environment, while the sp^2 hybridization between one s orbital and two p orbitals form three sp^2 orbitals. The sp^2 orbitals arrange themselves in a plane at 120° angle, hence forming a honeycomb lattice as seen in Fig. 1 [2, 7].

It is not classified as a Bravais lattice, since two neighbouring sites are not equivalent. This can be seen in Fig. 1 side A has a purple atom, and B holds green atoms. Hence, one can speak of two "sublattices", and the primitive unit cell contains two atoms as seen in Fig.1. Each sublattice alone is a triangular Bravais lattice on its own. Therefore, one can refer to the structure of graphene as a two-atom-based Bravais lattice.

The interatomic distance between two atoms of a sublattice is given by

$$\vec{a_1} = \frac{a}{2}(3, \sqrt{3}). \tag{1}$$

$$\vec{a_2} = \frac{a}{2}(3, -\sqrt{3}), \tag{2}$$

which are indicated in Fig. 1 on the LHS. The direct lattice vectors ($\vec{a_1}$ and $\vec{a_2}$) and the reciprocal lattice vectors ($\vec{b_1}$ and $\vec{b_2}$) satisfy the following equation:

$$\vec{a_i} \cdot \vec{b_j} = 2\pi\delta_{ij}. \tag{3}$$

Where δ_{ij} is the Dirac delta function. Plugging in the values for the direct vectors from Eqs. (1) and (2) into Eq. (3), we obtain a system of linear equations. Solving this yields the following expressions for the reciprocal lattice vectors:

$$\vec{b_1} = \frac{2\pi}{3a}(1, \sqrt{3}) \tag{4}$$

$$\vec{b_2} = \frac{2\pi}{3a}(1, -\sqrt{3}), \tag{5}$$

which are indicated in Fig. 1 on the RHS, as well as the vectors to the nearest neighbours of an atom, which may be useful to be defined. This is because it will be useful when it comes time to use the tight-binding Hamiltonian for graphene simply. The methods from [8] have been followed to define the three nearest neighbours that each atom can have:

$$\vec{\delta_1} = \frac{a}{2}(1, \sqrt{3}) \tag{6}$$

$$\vec{\delta_2} = \frac{a}{2}(1, -\sqrt{3}) \tag{7}$$

$$\vec{\delta_3} = a(-1, 0), \tag{8}$$

where a denotes the distance $a = 0.142nm$ between any nn atoms [5].

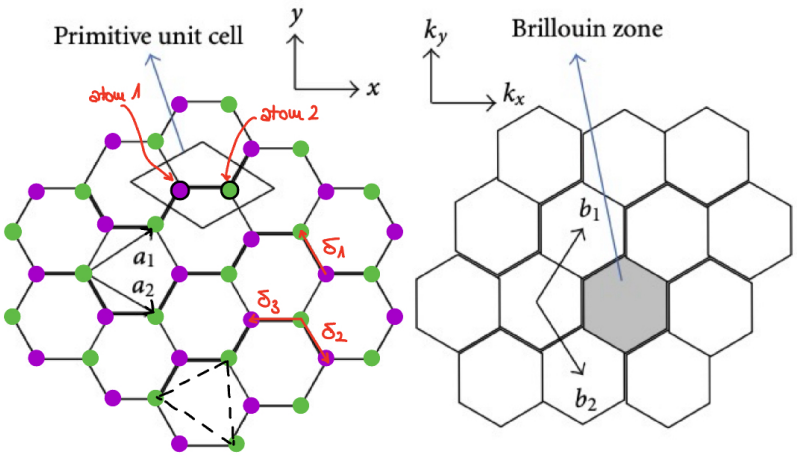

Figure 1: On the left side: shows the primitive lattice and vectors $\vec{a_1}, \vec{a_2}$, and the three nearest neighbours in $\vec{\delta_1}, \vec{\delta_2}, \vec{\delta_3}$. Furthermore, the two different atoms, green and purple, indicate the sublattices. The primitive unit cell containing two atoms, one green and one purple, is indicated. The dashed black lines denote the triangular Bravais lattice the sublattice builds by itself. On the right side, the grey filled-out space shows the first Brillouin zone and reciprocal vectors $\vec{b_1}, \vec{b_2}$ in k space. Obtained from [9].

Another important property in the graphene structure are the Dirac points $\vec{K}$ and $\vec{K'}$. They represent the inequivalent corners of the first Brillouin zone, as seen in Fig. 3. These points in the reciprocal lattice cannot be connected through a reciprocal lattice vector. The other four corners of the hexagonal structure of graphene can be reached from one of these Dirac points through translation by the reciprocal lattice vectors. These points will be relevant in further calculations and discussions since the low-energy excitations of graphene are centred around them, as seen in Sec. 2.4.

2.2 Tight-binding Model

We can now define the general tight-binding Hamiltonian, where we can have an electron hopping from site j to site ν and the reverse process. This is encoded in the following Hamiltonian:

$$H = -t \sum_{<j\nu>} a_j b_\nu^\dagger + a_j^\dagger b_\nu. \tag{9}$$

Where we have used the fermionic creation and annihilation operators a and $a^\dagger$ on site A and b and $b^\dagger$ on site B. The nature of the sites arises due to the symmetry of the hexagonal lattice. To simplify this problem further, we will consider nearest-neighbour hopping only with hopping contant t. The following notations of [8] have been used. We then obtain:

$$H = -t \sum_j \sum_\delta a_j b_{j+\vec{\delta}}^\dagger + b_j^\dagger a_{j+\vec{\delta}}. \tag{10}$$

Where we consider the three nearest neighbours $\delta_{1,2,3}$ and t is the nearest neighbour hopping potential. Then we consider the Fourier transforms of the creation and annihilation operators, which will make the Hamiltonian diagonal and remove offsite terms:

$$\begin{aligned}\hat{a}_j &= \frac{1}{\sqrt{N}}\sum_k \hat{a}_k e^{i\vec{k}.\vec{r}} \\ \hat{a}_j^\dagger &= \frac{1}{\sqrt{N}}\sum_k \hat{a}_k^\dagger e^{-i\vec{k}.\vec{r}}.\end{aligned} \tag{11}$$

Where $\vec{r}$ is the position vector and the operators are transformed into momentum space $\vec{k}$. This transformation can also be applied similarly for the B site operators. Substituting the Fourier transform in so that the off-diagonal elements of the Hamiltonian are eliminated and that we only consider on-site operators we obtain:

$$H = -\frac{t}{N}\sum_{k,k'}\sum_\delta a_k b_{k'}^\dagger e^{-i(\vec{k}-\vec{k'}).\vec{r}} e^{-i\vec{k'}.\vec{\delta}} + b_k^\dagger a_{k'} e^{i(\vec{k}-\vec{k'}).\vec{r}} e^{i\vec{k}.\vec{\delta}}. \tag{12}$$

Simplifying Eq.(13) by using the fact that $\sum_{k'} e^{i(\vec{k}-\vec{k'}).\vec{r}} = N\delta_{k,k'}$ we obtain:

$$\begin{aligned}H &= -t\sum_{k,k'}\sum_\delta a_k b_{k'}^\dagger e^{-i\vec{k'}.\vec{\delta}}\delta_{k,k'} + a_k^\dagger a_{k'} e^{i\vec{k}.\vec{\delta}}\delta_{k,k'} \\ &= -t\sum_k\sum_\delta b_k a_k^\dagger e^{-i\vec{k}.\vec{\delta}} + a_k^\dagger a_k e^{i\vec{k}.\vec{\delta}}.\end{aligned} \tag{13}$$

We can present this Hamiltonian in matrix notation:

$$H = -t\sum_k\sum_\delta \begin{pmatrix} a_k & b_k \end{pmatrix}\begin{pmatrix} 0 & \gamma_{\vec{k}}^* \\ \gamma_{\vec{k}} & 0 \end{pmatrix}\begin{pmatrix} a_k^\dagger \\ b_k^\dagger \end{pmatrix}. \tag{14}$$

We can obtain the dispersion relation from the determinant of the matrix which will be given by $\epsilon(\vec{k}) = -t\sqrt{\gamma_{\vec{k}}\gamma_{\vec{k}}^*}$ (this won't trivially be equal to unity as we will see) and $\gamma_{\vec{k}} = e^{i\vec{k}.\vec{\delta}}$.

To calculate the dispersion relation, we will write out the exponential explicitly:

$$\begin{aligned}\sum_\delta e^{i\vec{k}.\vec{\delta}} &= e^{i\vec{k}.\vec{\delta_1}} + e^{i\vec{k}.\vec{\delta_2}} + e^{i\vec{k}.\vec{\delta_3}} \\ &= e^{i\frac{a}{2}(k_x+\sqrt{3}k_y)} + e^{i\frac{a}{2}(k_x-\sqrt{3}k_y)} + e^{iak_x} \\ &= e^{iak_x}[1 + e^{-i\frac{a}{2}k_x}(e^{i\frac{a}{2}\sqrt{3}k_y} + e^{-i\frac{a}{2}\sqrt{3}k_y})] \\ &= e^{iak_x}[1 + 2e^{-i\frac{a}{2}k_x}\cos\frac{\sqrt{3}}{2}k_y a].\end{aligned} \tag{15}$$

The dispersion relation can be calculated now because it will only depend on k_x, k_y. we can define $\epsilon(\vec{k}) = \epsilon(k_x, k_y)$:

$$\epsilon(k_x,k_y) = \pm t\sqrt{1 + 4\cos(\frac{3}{2}k_x a)\cos(\frac{\sqrt{3}}{2}k_y a) + 4\cos^2(\frac{\sqrt{3}}{2}k_y a)}. \tag{16}$$

As we can see, There are two solutions. This will correspond to 2 bands in graphene's dispersion as seen in Fig. 2, where it is plotted as a function of k_x and k_y.

The positive sign corresponds to the conduction band, and the negative sign corresponds to the valence band. Another interesting fact is that the band gap will be zero, leading to interesting properties, which will be discussed in further detail.

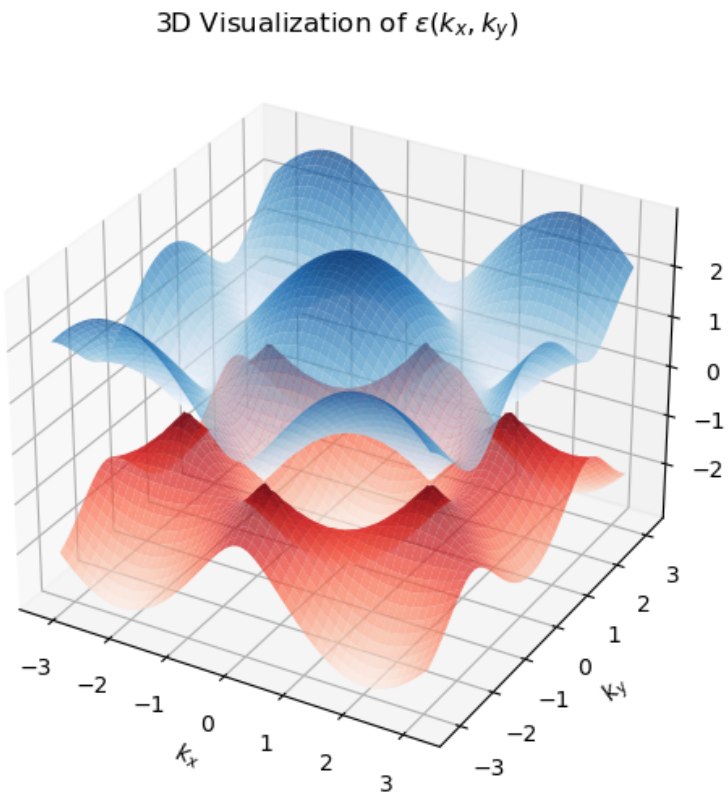

Figure 2: Dispersion relation of graphene on the z-axis $\epsilon(\vec{k})$, as a function of the momentum space in the first Brillouin zone on the x and y-axis k_x, k_y. The band gap decreases to zero at the Dirac points.

2.3 Metal, Insulator vs semi-conductor

Since we have obtained the valence and conduction bands of graphene, we can analyse where the Fermi energy lies and deduct the conductive behaviour of this system. Each carbon atom will provide one free electron [10]. In the primitive unit cell, there are two atoms. If each carbon atom contributes one electron, then there will be two free electrons per unit cell. Since each electron fills half of a band, graphene will fully fill its conductive (bottom) band. Graphene can be considered a semiconductor if the band gap is smaller than 4 eV; if the band gap is larger, it will be an insulator. However, from Fig. 2, we can see that the energy gap is zero at the Dirac points (Fig. 3). This will mean that graphene will be a conductor. Extending this further, it can be seen that graphene is a superconductor! There will be no energy cost to transfer between the valence and conduction band.

2.4 Low energy limit

In this section, we aim to obtain the expression for the tight-binding Hamiltonian and the band dispersion near the Fermi level in the limit of small wave vectors with respect to the Fermi wave vector. Expanding the Hamiltonian for wavevectors near the wavevector corresponding to the Fermi energy is a low-energy expansion.

In graphene due to graphene's unique electronic band structure, it is characterized by Dirac points at $\vec{K}$ and $\vec{K}'$ at the corners of the Brillouin zone, which can be seen in Fig. 3. The Dirac points are positions within the Brillouin zone where the energy dispersion relation intersects with the Fermi level.

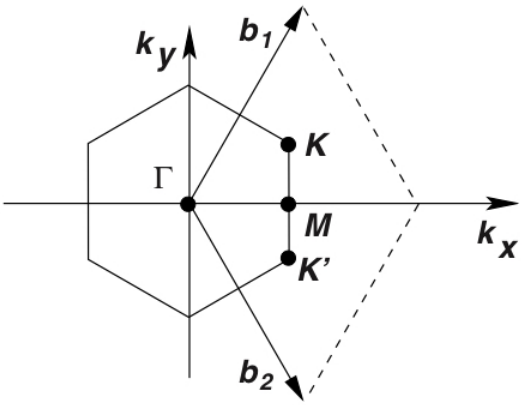

Figure 3: The first Brillouin zone of the Graphene, indicated by a solid line, with its centre Γ. The Dirac cones are located at the $\vec{K}$ and $\vec{K}'$ points. Figure taken from [2].

In graphene, the energy dispersion relation for the electrons follows a linear relationship near these Dirac points, resembling the dispersion relation of massless Dirac fermions, as we will see in Sec. 2.5, in Fig 4. At $\vec{K}$ and $\vec{K}'$ the conduction and valence bands touch each other, resulting in a zero bandgap, which can be observed in Fig. 4. This means that the energy of the electrons at these points is the same as the Fermi level. Consequently, the Fermi level intersects with the energy dispersion relation precisely at the Dirac points in graphene. At $\vec{K}$ and $\vec{K}'$, we would obtain zero energy for massless Dirac fermions, which is shown in Fig. 4. To start this problem, we consider the effective tight-binding Hamiltonian [5]

$$H \equiv t \begin{pmatrix} 0 & \gamma_{\vec{k}}^* \\ \gamma_{\vec{k}} & 0 \end{pmatrix} + t_{nnn} |\gamma_{\vec{k}}|^2 \begin{pmatrix} 1 & 0 \\ 0 & 1 \end{pmatrix}, \tag{17}$$

where $\gamma_{\mathbf{k}}$ is a phase factor and t is the nearest neighbour hopping parameter, and t_{nnn} the next-nearest neighbour hopping parameter. While this Hamiltonian shows contributions for the next nearest neighbour contributions, in the actual expansion in the low-energy region, we will restrict ourselves to nearest neighbour contributions as we omit the *nnn* hopping corrections. We only restrict ourselves to a first-order expansion, such that $\mathcal{O}(|\gamma_{\mathbf{k}}|^2)$.

The characteristic energy of low-energy excitations is significantly smaller than the bandwidth $\sim |t|$, so it can be restricted to excitations at the Fermi level. This means the quantum states can be restricted to within the vicinity of the Dirac points, and the energy dispersion is expanded around $\pm\vec{K}$, where the + denotes the conduction band and the − the valence band. Hence, the wavevector can be decomposed as $\vec{k} = \pm\vec{K} + \vec{q}$, where $|q| \ll |\vec{K}| \sim 1/a$. The governing parameter of expansion

of the energy dispersion then becomes $|\vec{q}|a \ll 1$.

It is important to note that in this paragraph, we rotated the $\vec{a_2}$ by 180° to read: $\vec{a_2} = \frac{a}{2}(-3, \sqrt{3})$, $\vec{a_1}$ remains the same. We define the sum of the phase factors of the nn contribution as

$$\gamma_{\vec{k}} \equiv 1 + e^{i\vec{k}\cdot\vec{a_1}} + e^{i\vec{k}\cdot\vec{a_2}}. \tag{18}$$

Lastly, we need to find $\vec{K}$ to later evaluate the dot product $\vec{K}\cdot\vec{a_i}$, where $i = 1, 2$ as in Eq. (18) $\vec{k}$ is decomposed into $\vec{k} = \pm\vec{K} + \vec{q}$. The full derivation for $\vec{K}$ is given in appendix A. To simplify the above-found Hamiltonian, the phase factors $\gamma_{\vec{k}}$ need to be expanded with the decomposed wave vector, as follows,

$$\begin{aligned}
\gamma_{\vec{q}}^{\pm} \equiv \gamma_{\vec{k}=\pm\vec{K}+\vec{q}} &= 1 + e^{\pm i\vec{K}\cdot\vec{a}_1} e^{i\vec{q}\cdot\vec{a}_1} + e^{\pm i\vec{K}\cdot\vec{a}_2} e^{i\vec{q}\cdot\vec{a}_2} \\
&\simeq 1 + e^{\pm i2\pi/3}\left[1 + i\vec{q}\cdot\vec{a}_1 - \frac{1}{2}(\vec{q}\cdot\vec{a}_1)^2\right] + e^{\mp i2\pi/3}\left[1 + i\mathbf{q}\cdot\vec{a}_2 - \frac{1}{2}(\vec{q}\cdot\vec{a}_2)^2\right] \\
&= \gamma_{\vec{q}}^{\pm(0)} + \gamma_{\vec{q}}^{\pm(1)} + \gamma_{\vec{q}}^{\pm(2)}.
\end{aligned} \tag{19}$$

Dirac points and their positions at the BZ corners K and K' give $\gamma_{\vec{q}}^{\pm(0)} = \gamma_{\pm\vec{K}} = 0$. As we will limit the expansion to first order in $|\vec{q}|a$, such that $\mathcal{O}(\vec{q}\cdot\vec{a})^2$, we only further investigate $\gamma_{\vec{q}}^{\pm(1)}$. If we expand $|\vec{q}|a$ in first order in 2D such that $\vec{q}$ is has its components along x and y we get,

$$\begin{aligned}
\gamma_{\vec{q}}^{\pm(1)} &= i\frac{\sqrt{3}a}{2}\left[(q_x + \sqrt{3}q_y)e^{\pm i2\pi/3} + (-q_x + \sqrt{3}q_y)e^{\mp i2\pi/3}\right] \\
&= \mp\frac{3a}{2}(q_x + iq_y),
\end{aligned} \tag{20}$$

utilizing $\sin(\pm 2\pi/3) = \pm\sqrt{3}/2$ and $\cos(\pm 2\pi/3) = -1/2$. Putting this back into the Hamiltonian given in Eq. (17), we obtain,

$$H_{\vec{q}}^{\text{eff},\xi} = -\xi\frac{3ta}{2}\begin{pmatrix} 0 & q_x - i\xi q_y \\ q_x + i\xi q_y & 0 \end{pmatrix}. \tag{21}$$

Above the valley isospin is defined as $\xi = \pm$, where $\xi = +$ refers to the K point at $+\vec{K}$ and $\xi = +$ refers to the K' point at $-\vec{K}$. Defining the Fermi velocity as $v_F \equiv -3ta/2$. Such that we can rewrite the Hamiltonian as [5]

$$H_{\vec{q}}^{\text{eff},\xi} = \xi v_F(q_x\sigma_x + \xi q_y\sigma_y), \tag{22}$$

where σ_x, σ_y refers to the Pauli matrices. The energy dispersion is then given as

$$\epsilon_{\vec{q}}^{\xi=\pm} = \pm\hbar v_F|\vec{q}|, \tag{23}$$

which is independent of the valley isopin ξ.

The dispersion at low energies resembles the structure of quantum electrodynamics (QED) for massless fermions, with the primary difference that in Graphene, the Dirac fermion moves with v_F, which is ~ 300 times smaller than c [2, 7]. This leads to QED properties being displayed by Graphene but at much smaller speeds.

2.5 Density of States

To investigate how the electrons behave at low energy excitations, we will look closely at the density of states in the limit of small wave vectors. In order to do that, we must firstly have to look at the dispersion relation close to the Dirac points, hence where $\vec{q} = \vec{k} - \vec{K}$ goes to zero. In the vicinity of the Dirac points, the energy bands are therefore described by a linear dispersion relation:

$$\epsilon_{\pm} = \pm \hbar v_F |\vec{q}|. \tag{24}$$

Again, the + corresponds to the conduction band and the − to the valence band. The energy

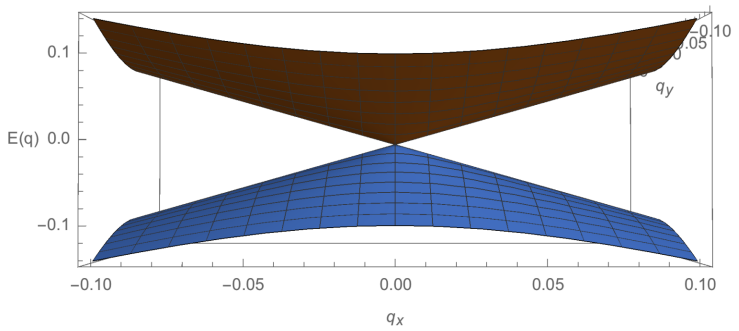

Figure 4: Dispersion relation of graphene in the low wavevector limit, E(q), against the wave vector q_x. In close proximity to the Dirac points ($q_x, q_y = 0$), the dispersion relation is linear in momentum, such that the energy bands form a cone, which is referred to as a Dirac cone. Obtained from [8].

bands each form a cone with the vertex lying at the Dirac point, as shown in Fig. 4.

In general, the density of states is directly related to the number of available energy levels that an electron can occupy and is defined in the following way in the 2-dimensional case:

$$D(\epsilon) = \frac{1}{A} \sum_k \delta(\epsilon - \epsilon_k), \tag{25}$$

where A is the area of the real lattice. We replace the momentum vector $\vec{k}$ with the relative momentum vector $\vec{q}$. Furthermore, we will replace the sum by an integral (which is symmetric due to the structure). This leads to the following expression:

$$D(\epsilon) = \frac{1}{A} \frac{A}{(2\pi)^2} 2 \int_0^{\infty} \delta(\epsilon - \epsilon_q) 2\pi q dq \tag{26}$$

$$= \frac{1}{\pi} \int_0^{\infty} \delta(\epsilon - \epsilon_q) q dq. \tag{27}$$

Here we used that the reciprocal area (in k-space) occupied by one state is $\frac{2\pi^2}{A}$. Using the dispersion relation given by Eq. (25), we can express the relative momentum in terms of the energy:

$$d\epsilon_{\pm} = \pm \hbar v_F dq,$$

and hence

$$\epsilon d\epsilon = \hbar^2 v_F^2 q dq.$$

Note that due to the multiplication, the $\pm$ disappears, and we have a degeneracy of $g_v = 2$ as there are two Dirac points which we have to regard in further calculations (as seen in [11]).
This leads to the following expression for the density of states:

$$D(\epsilon) = \frac{g_v}{\pi\hbar^2 v_F^2} \int_0^\infty \delta(\epsilon - \epsilon_q)\epsilon_q d\epsilon_q, \tag{28}$$

which leaves us with a simple integral over a delta function. Computing this leads us to the density of states for the bands of graphene in the limit of small wave vectors:

$$D(\epsilon) = \frac{2|\epsilon|}{\pi\hbar^2 v_F^2}. \tag{29}$$

Apart from using the sum of the density state of all possible k, we can also calculate the density of states for the total number of states:

$$N(k)dk = \frac{2\pi k dk}{\left(\frac{2\pi}{L_x}\right)\left(\frac{2\pi}{L_y}\right)} g_s g_v, \tag{30}$$

where $N(k)$ is the number of states of k. L_x and L_y are crystal sizes in real space and g_s is represented for spin degeneracy, which is equal to 2 in graphene. Then, we can use the energy dispersion of Fermi energy:

$$N(k)dk = 2A\frac{kdk}{\pi} = 2A\frac{\epsilon d\epsilon}{\pi(\hbar v_F)^2}. \tag{31}$$

Then we can have the density of state per A and per ϵ and consider $v_F \equiv -3ta/2$:

$$D(\epsilon) = \frac{2\epsilon}{\pi\hbar^2 v_F^2} \equiv \frac{g_s \cdot g_v}{2\pi}\frac{|\epsilon|}{\hbar^2 v_F^2} = \frac{8\,|\epsilon|}{9\pi a^2\hbar^2 t^2}, \tag{32}$$

which has the same form as (29).

3 Boron Nitride

Boron Nitride, specifically 2D hexagonal boron nitride, has a crystal structure similar to that of graphene. B (boron) and N (nitrogen) atoms are alternately arranged in a honeycomb structure. Three orbits of each boron atom combine with a nitrogen atom's sp^2 orbit to form a strong covalent chemical bond. On the other hand, different layers of boron nitride are held together by weak Van der Waals forces [12]. Unlike graphene, boron nitride exhibits high-temperature stability, a low dielectric constant, and high thermal conductivity. Because of these and other properties, it is often used together with graphene as an insulating layer or to improve the performance of graphene devices in conditions such as higher temperatures or higher electric fields [12].
In the following, we shall explore the tight-binding Hamiltonian assuming that there is one (p_z) orbital on each atomic site and that there is hopping only between the nearest-neighbour sites. Furthermore, we have to take into account that the onsite energies of B and N are different.

3.1 The 2D Boron Nitride Lattice

Figure 5 shows the hexagonal lattice of boron nitride. The purple atoms represent boron, and the blue atoms represent nitrogen. The arrows a_1 and a_2 display the lattice vectors and point to the

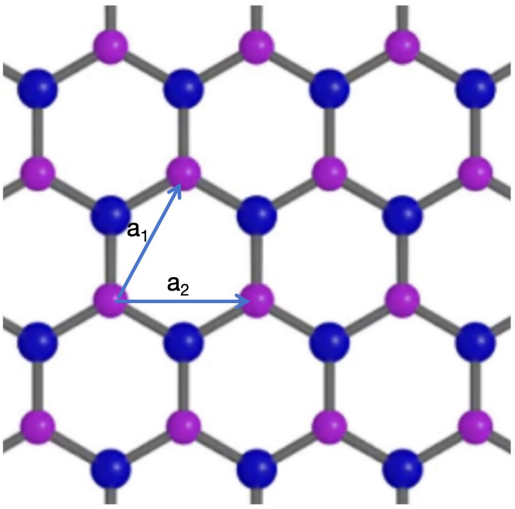

Figure 5: 2D hexagonal boron nitride: Purple atoms represent boron, and blue atoms represent nitrogen. a_1 and a_2 are the primitive lattice vectors

nearest neighbours.

In 2D h-BN, we use a new lattice vector to make it easier to describe Hamiltonian.

$$\vec{a_1} = \frac{a}{2}(\sqrt{3}, 3) \tag{33}$$

$$\vec{a_2} = \frac{a}{2}(\sqrt{3}, 0). \tag{34}$$

3.2 Tight-Binding Hamiltonian in Boron Nitride

Assuming that the onsite energy for B and N atoms are ϵ_B and ϵ_N, respectively. The Hamiltonian for the onsite part is

$$H_0 = \sum_r \epsilon_s a^\dagger_{r,s} a_{r,s}, \tag{35}$$

where $a^\dagger_{r,s}$ and $a_{r,s}$ are the fermionic creation and annihilation operators for the electron at the unit cell located at $r = ma_1 + na_2$ and on the sublattice s (B or N atoms). The sketch of lattice basis vectors is depicted in Fig. 5. In a honeycomb lattice, it means that an atom will interact only with its three nearest neighbours [13], so the hopping part of the Hamiltonian takes the form of

$$H_1 = -t_{BN} \sum_r \left(a^\dagger_r a_{r+a_1} + a^\dagger_{r+a_1} a_{r+a_1} + a^\dagger_{r+a_2} a_{r+a_1} \right) + H.c.$$

where t_{BN} is the hopping integral between the adjoint N and B atoms. Collecting the above two parts, we have

$$H = \sum_{r,s=B/N} \epsilon_s a^\dagger_{r,s} a_{r,s} - t_{BN} \sum_r \left(a^\dagger_r a_{r+a_1} + a^\dagger_{r+a_1} a_{r+a_1} + a^\dagger_{r+a_2} a_{r+a_1} \right) + H.c.$$

Above $s = B/N$ means that s can take B or N.

3.3 Band Dispersion of Electrons in 2D Boron Nitride

To calculate the band dispersion, we take periodic boundary conditions in both directions and make the Fourier expansion as

$$a_{r,s} = \frac{1}{\sqrt{L_x L_y}} \sum_k a_{k,s} e^{-i\vec{k}\cdot\vec{r}}$$

$$a^\dagger_{r,s} = \frac{1}{\sqrt{L_x L_y}} \sum_k a^\dagger_{k,s} e^{i\vec{k}\cdot\vec{r}},$$

where L_x and L_y are the length in x and y directions. For the onsite part, we have

$$H_0 = \frac{1}{L_x L_y} \sum_{r,s=B/N} \sum_{k,k'} \epsilon_s a^\dagger_{k,s} e^{i\vec{k}\cdot\vec{r}} a_{k',s} e^{-i\vec{k'}\cdot\vec{r}}.$$

Using the orthogonal relation

$$\frac{1}{L_x L_y} \sum_r e^{i(\vec{k}-\vec{k'})\cdot\vec{r}} = \delta_{k,k'},$$

we have

$$H_0 = \sum_{k,s} \epsilon_s a^\dagger_{k,s} a_{k,s}.$$

For the hopping part, we have

$$\begin{aligned} H_1 &= -t_{BN} \sum_r \left(a^\dagger_r a_{r+a_1} + a^\dagger_{r+a_1} a_{r+a_1} + a^\dagger_{r+a_2} a_{r+a_1} \right) + H.c. \\ &= -t_{BN} \sum_k a^\dagger_k a_k \left(e^{-ik\cdot a_1} + 1 + e^{-ik\cdot(a_1-a_2)} \right) + H.c. \end{aligned} \tag{36}$$

Once again, defining the eigenstates as we did before

$$\Psi_k = \begin{pmatrix} a^\dagger_{k,N} \\ a^\dagger_{k,B} \end{pmatrix}. \tag{37}$$

We have

$$H = \sum_k \psi^\dagger_k h(k) \psi_k = \sum_k \psi^\dagger_k \begin{pmatrix} \epsilon_N & f_k \\ f^*_k & \epsilon_B \end{pmatrix} \psi_k$$

$$f_k = 1 + e^{-i\vec{k}\cdot\vec{a_1}} + e^{-i\vec{k}\cdot(\vec{a_1}-\vec{a_2})},$$

and the band dispersion is solved from

$$\det\left[\epsilon\, I_{2x2} - h(k)\right] = 0,$$

from which we obtained that

$$\epsilon_k = \epsilon_0 \pm \sqrt{\Delta^2 + |f_k|^2}$$

$$= \epsilon_0 \pm \sqrt{\Delta^2 + 3 + 2\cos\left(\frac{\sqrt{3}}{2} k_x a\right) + 4\cos\left(\frac{\sqrt{3}}{2} k_x a\right) \cos\left(\frac{3}{2} k_y a\right)},$$

which has a similar form as [13] where

$$\epsilon_0 = \frac{\epsilon_N + \epsilon_B}{2}, \quad \Delta = \frac{\epsilon_N - \epsilon_B}{2}.$$

Similar to graphene, hopping only happens with the three nearest neighbours in the h-BN. It also has two bands for conduction and valence. Compared to graphene, the energy bands of boron nitride are shifted by ϵ_0 due to the difference in electronic structure, and its structure has a band gap which is equal to Δ at K and K' points in the 1st BZ. There is only one p_z orbital per site (one free electron per site). Given that there are 2 free electrons per unit cell so that the Fermi energy lies similar to that in graphene, this band gap means that it will not have superconductor capabilities like graphene. As the band gap is ≈ 5 eV [14], boron nitride will act as a large gap semiconductor.

4 Conclusion

In this report, we present the 2D hexagonal lattice of graphene. We have shown that it will have two sub sites due to its symmetry. We then presented the tight-binding Hamiltonian, and Fourier transformed it to eliminate the offsite terms and make the Hamiltonian diagonal. We then adapt the diagonal Hamiltonian to the geometry of the hexagonal lattice and find the dispersion relation. The dispersion relation has a zero band gap at the Dirac points and resembles massless free fermions in the low wavevector limit. Then, we presented the h-BN lattice. The difference is that there will be alternating boron and nitrogen atoms instead of repetitive carbon positioning. The dispersion relation is calculated, and a band gap appears between the two bands of hBN.

The most significant difference between graphene and boron nitride is the structure of the energy bands. The two energy bands (valence and conduction) of graphene have a structure which is shown in Fig. 2 and for the low wave vector limit in Fig. 4. The two energy bands touch and therefore there is no energy gap, therefore graphene is a zero band gap superconductor. On the other hand, boron nitride exhibits a different band dispersion, shown in Eq. 3.3. The energy bands are shifted by ϵ_0, and boron nitride is considered a large gap semiconductor with a band gap of ≈ 5 eV.

The structures of these materials are very similar. Therefore, it is not far from intuition to combine these two materials and see the outcome[15]. One way to combine these materials is to add layers of these materials is and by changing the relative alignment and rotation of the two layers. The effect of this is that the optical and electronic properties of the original graphene (bi)layer are altered. Adding boron nitride can introduce secondary Dirac points [14]. These 2D materials with strong inter-molecular attraction forces and weak inter-layer forces are called van der Waals (vdW) materials, and there are many other examples, e.g. MoS_2 (semiconductor) and $NbSe_2$ (superconductor) of these vdW materials. Combining these materials in different ways can change the strength and optical and electronic properties.

References

[1] Kartika A. Madurani and Suprapto. Progress in Graphene Synthesis and its Application: History, Challenge and the Future Outlook for Research and Industry. *ECS J. Solid State Sci. Technol.*, 9(9):093013, October 2020.

[2] A. H. Castro Neto, F. Guinea, N. M. R. Peres, K. S. Novoselov, and A. K. Geim. The electronic properties of graphene. *Rev. Mod. Phys.*, 81(1):109–162, January 2009.

[3] C. N. R. Rao, Kanishka Biswas, K. S. Subrahmanyam, and A. Govindaraj. Graphene , the new nanocarbon. *J. Mater. Chem.*, 19(17):2457–2469, 2009.

[4] Santosh K. Tiwari, Sumanta Sahoo, Nannan Wang, and Andrzej Huczko. Graphene research and their outputs: Status and prospect. *J. Sci.: Adv. Mater. Devices*, 5(1):10–29, March 2020.

[5] J. Fuchs and M. Goerbig. Introduction to the Physical Properties of Graphene, 2008. [Online; accessed 15. Mar. 2024].

[6] Cory R Dean, Andrea F Young, Inanc Meric, Chris Lee, Lei Wang, Sebastian Sorgenfrei, Kenji Watanabe, Takashi Taniguchi, Phillip Kim, Kenneth L Shepard, et al. Boron nitride substrates for high-quality graphene electronics. *Nature nanotechnology*, 5(10):722–726, 2010.

[7] Anthony J. Leggett, January 2015. [Online; accessed 14. Mar. 2024].

[8] Franz Utermohlen. Tight-Binding Model for Graphene. *Lect. Note*, 9:12, 2018.

[9] Davood Fathi. A Review of Electronic Band Structure of Graphene and Carbon Nanotubes Using Tight Binding. *J. Nanotechnol.*, 2011(20), January 2011.

[10] Anthony Gerges Geha, Yago aguado, and Modou B. Nadiaye. Graphene, a material with exceptional electronic properties, 2024.

[11] Professor Mark Lundstrom Electrical and West Lafayette Computer Engineering Purdue University. ECE-656: Fall 2011 Lecture 3: Density of States. Lecture of Purdue University, West Lafayette, August 2011. [Online; accessed 10. Mar. 2024].

[12] Jingang Wang, Fengcai Ma, and Mengtao Sun. Graphene, hexagonal boron nitride, and their heterostructures: properties and applications. *RSC Adv.*, 7(27):16801–16822, March 2017.

[13] Paul Giraud. *Study of the Electronic Structure of hexagonal Boron Nitride on Metals Substrates*. PhD thesis, Master Thesis, Université des Sciences et Technologies Lille 1, 2012.

[14] G. Cassabois, P. Valvin, and B. Gil. Hexagonal boron nitride is an indirect bandgap semiconductor. *Nat. Photonics*, 10:262–266, April 2016.

[15] A. K. Geim and I. V. Grigorieva. Van der Waals heterostructures. *Nature*, 499:419–425, July 2013.

A Derivation of the position of $\vec{K}$

The derivation follows the Derivation in [5]. The Dirac points are situated at the points $\vec{k}^D$ where the energy dispersion of the Hamiltonian containing next-nearest neighbour and nearest neighbour contributions is zero. The energy dispersion of nn and nnn contributions is zero when

$$\epsilon_{\vec{k}} = 2t_{nnn}\sum_{i=1}^{3}\cos(\vec{k}\cdot\vec{a_i}) + \pm t\sqrt{3+2\sum_{i=1}^{3}\cos(\vec{k}\cdot\vec{a_i})} = 0. \tag{38}$$

This is satisfied when $\gamma_{\vec{k}^D} = 0$. Using Eq. (18) and investigating the real and imaginary parts of $\gamma_{\vec{k}^D}$ we find,

$$\begin{aligned}\mathrm{Re}(\gamma_{\vec{k}^D}) &= 1 + \cos(\vec{k}^D\cdot\vec{a_1}) + \cos(\vec{k}^D\cdot\vec{a_2}) \\ &= 1 + \cos\left[\frac{\sqrt{3}a}{2}(k_x^D + \sqrt{3}k_y^D)\right] + \cos\left[\frac{\sqrt{3}a}{2}(-k_x^D + \sqrt{3}k_y^D)\right] = 0.\end{aligned} \tag{39}$$

Similarly, for the imaginary part:

$$\mathrm{Im}(\gamma_{\vec{k}^D}) = \sin\left[\frac{\sqrt{3}a}{2}(k_x^D + \sqrt{3}k_y^D)\right] + \sin\left[\frac{\sqrt{3}a}{2}(-k_x^D + \sqrt{3}k_y^D)\right] = 0. \tag{40}$$

The equation may be satisfied when $k_y^D = 0$, such that

$$1 + 2\cos\left(\frac{\sqrt{3}a}{2}\vec{k}_x^D = 0\right). \tag{41}$$

This is the case the Dirac points at

$$\vec{k}^D = \pm\vec{K} = \pm\frac{4\pi}{3\sqrt{3}a}\hat{x} \tag{42}$$

.